

# Ground-Motion Prediction Equations (GMPEs) from a Global Dataset: The PEER NGA Equations

David M. Boore

U.S. Geological Survey

## Abstract

The PEER NGA ground-motion prediction equations (GMPEs) were derived by five developer teams over several years, resulting in five sets of GMPEs. The teams used various subsets of a global database of ground motions and metadata from shallow earthquakes in tectonically active regions in the development of the equations. Since their publication, the predicted motions from these GMPEs have been compared with data from various parts of the world—data that largely were not used in the development of the GMPEs. The comparisons suggest that the NGA GMPEs are applicable globally in tectonically active regions.

## Introduction

The Pacific Earthquake Engineering Research (PEER) Center conducted a multi-year project (the “Next Generation Attenuation (NGA)” project) to derive ground-motion prediction equations (GMPEs, to use a term coined in Appendix A of Boore and Atkinson, 2007) from data collected globally in active tectonic regions. Detailed descriptions of the project and the GMPEs are readily available in a special issue of *Earthquake Spectra* (volume 24, No. 1), as well as other papers, such as Campbell et al. (2009), and for that reason this article only gives a capsule description of the essential details of the NGA project. New to this article will be a number of figures not contained in the *Earthquake Spectra* special issue. Because of length limitations, this article will primarily be composed of extended figure captions.

## **The NGA-Empirical Project**

### ***Personnel***

The new GMPEs were derived by five developer teams: Abrahamson and Silva (AS), Boore and Atkinson (BA), Campbell and Bozorgnia (CB), Chiou and Youngs (CY), and Idriss (I). Because the Idriss GMPEs are of limited use (they are only for rock sites), they will not be discussed in this article. A number of working groups performed studies in support of the derivation of the GMPEs (see Power et al., 2008, for details).

### ***Scope***

The developer teams were given the task of developing GMPEs for a median measure of ground motion (“*GMRot150*”, as defined in Boore et al., 2006; see Beyer and Bommer, 2006; Campbell and Bozorgnia, 2007; Watson-Lamprey and Boore, 2007; and Huang et al., 2008, provided equations to convert *GMRot150* to maximum spectral amplitude), including peak acceleration, velocity, and displacement, as well as 5%-damped pseudo spectral acceleration (PSA) for periods from 0.01 s to 10 s. The equations were to be valid for magnitudes ranging from 5.0-8.5 (for strikeslip faulting) and 5.0-8.0 for reverse slip faulting) and distances from 0 to 200 km. Models for the aleatory variability were to be included.

### ***Database***

A major effort was put into developing the database to be used by the developers (see Chiou et al., 2008, for details). Generally, the data are from shallow earthquakes located in tectonically active, shallow lithosphere, with reliable earthquake metadata being available.

## Model Development

### *Dataset Selection*

The developers used subsets of the full database, with justifications for the data not used. For example, BA excluded data from aftershocks, records for which metadata were missing or for which only one horizontal component was available, non “free-field” installations, etc. Figure 1 shows the magnitude-distance distribution of data for *pga* and for *PSA* at  $T=10.0$  s period. Note that there are many fewer data at longer periods than at shorter periods, a natural consequence of the low-cut filtering used in processing the data. Also note that there are no normal-fault data for  $T=10.0$  s. For these reasons, the GMPEs at longer periods (and for normal faults) will be less certain than at shorter periods.

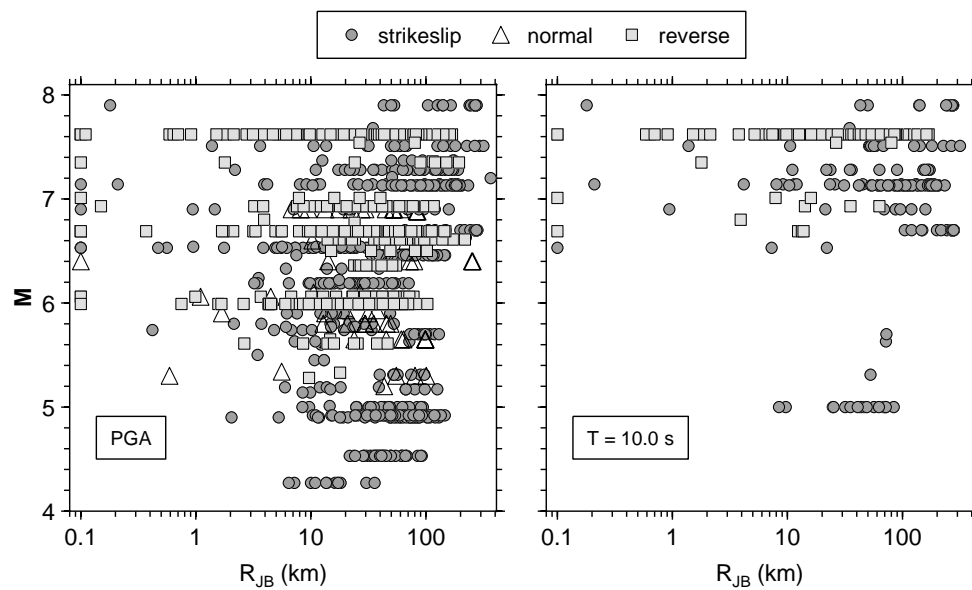


Figure 1. Magnitude and distance distribution of data used by BA. Each symbol represents a recording.

## ***Functional Forms***

Each developer team chose different functional forms for the GMPEs, in order to capture effects that they thought should be modeled. The functional forms are a tradeoff between simplicity of use and being able to represent the complexity in ground motions, due to many physical effects. Some of the effects captured in the functional forms are given below, as divided into source, path, and site contributions:

### **Source**

- Fault mechanism (all developers)
- Aftershock vs mainshock (AS, CY; aftershocks not used by BA, CB)
- Depth to top of rupture ( $Z_{TOR}$ ) (all but BA)
- Magnitude scaling (all, different functions)
- Radiation pattern (not included)
- Directivity (not included)

### **Path**

- Near-source (effect of fault size--CY)
- Far-source
  - Geometric spreading (single or multisegment (CY),  $M$  (moment magnitude) dependent (all but CY))
  - Anelastic attenuation (included by all but CB,  $M$  dependent in CY)
  - Source-site geometry (“hanging wall effect”) (all but BA)

### **Site**

- Near-surface geology (all)
  - Linear
  - Nonlinear
- Sediment thickness (“basin depth”; all but BA)

### **Aleatory Variability**

- Inter (between) event ( $\tau$ )
- Intra (within) event ( $\sigma$ ): usually larger
- Dependence on  $M$  and/or rock reference-level motion? All but BA, but with different functions. Reduction of variance on soil sites for larger rock input motions makes physical sense.

The effects to be captured by the GMPEs were usually determined by a combination of exploratory data analysis and, for effects for which the recorded data are not sufficient to determine the effects, theoretical considerations. An example of the need for saturation in motions at short periods as magnitude increases is given in Figure 2.

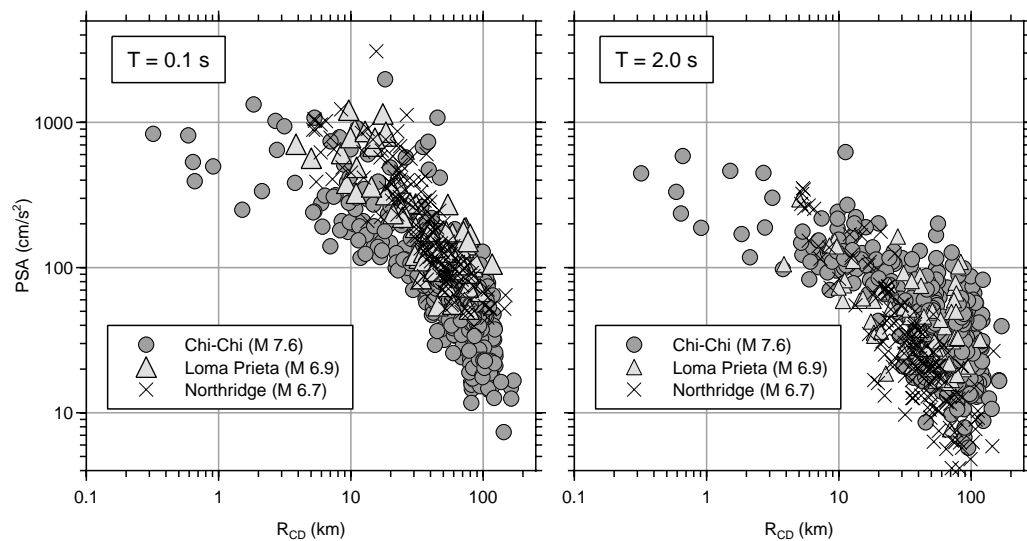


Figure 2. Ground motions for three earthquakes for two oscillator periods. Note that the motions from the M 7.6 Chi-Chi earthquake are smaller and larger than for the smaller earthquakes at short and long period, respectively.

In all but the Idriss GMPEs, the site response is considered to be nonlinear. Because the amount of nonlinearity and the amplitude of the site response are functions of both period and the  $V_{S30}$  (the variable chosen to characterize the site), the functional forms required to account for these effects are generally complex. Figure 3 shows the site response for the BA equations, clearly showing the nonlinear site response.

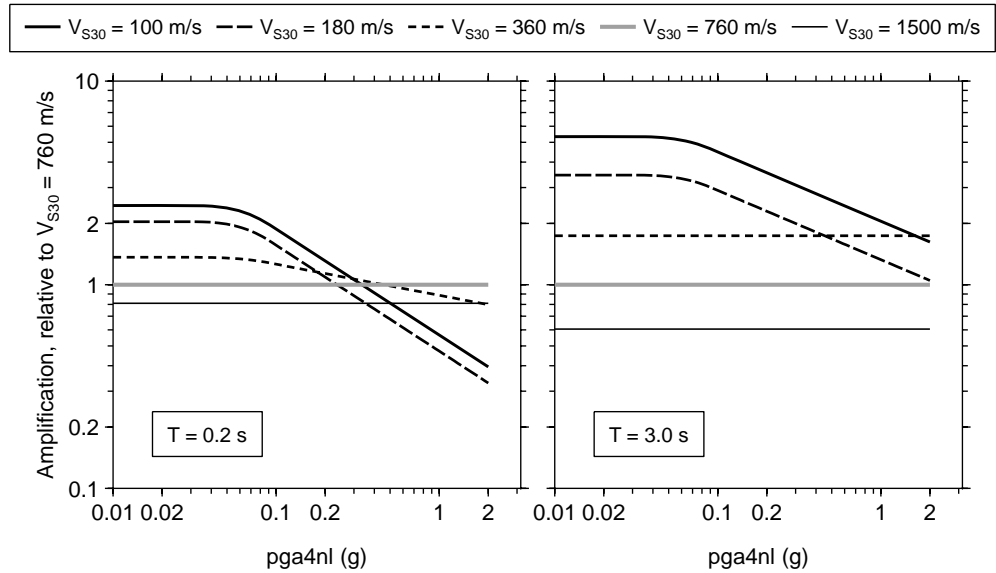


Figure 3. Site response for the BA GMPEs. Note the larger amplifications for long periods and the nonlinear response at both periods, particularly for softer sites.

As with site amplification, capturing a number of the physical effects requires complex GMPEs. This is a necessary consequence of going beyond simple magnitude, distance, and scalar site effects as predictor variables.

Table 1 summarizes the effects included in the GMPEs for the various developer teams.

Table 1. Effects included in the GMPEs of the NGA developer teams.

Effect	AS08	BA08	CB08	CY08	I08
Saturation at short distances	X	X	X	X	X
Style-of-faulting	X	X	X	X	X
Rupture depth factor	X		X (RV only)	X	
Hanging wall factor	X		X	X	
Nonlinear site amp	X	X	X	X (emp)	
Sed. Depth factor	X		X	X (emp)	
$M$ -dependent $\sigma$	X			X	X

Nonlinear effects on $\sigma$	$\sigma, \tau$		$\sigma$	$\sigma, \tau$	
-------------------------------	----------------	--	----------	----------------	--

“emp”=based on analysis of empirical data; “RV”= reverse-slip fault

The predictor variables in the GMPEs include the following:

- $M$  = Moment magnitude
- $R_{RUP}$  = Closest distance to coseismic rupture (km)
- $R_{JB}$  = Closest distance to surface projection of coseismic rupture (km)
- $R_x$  = Horizontal distance from top edge of fault perpendicular to strike (km)
- $Z_{TOR}$  = Depth to top of coseismic rupture (km)
- Fault type (depends on rake or P, T plunges)
- $F_{AS}$  = 1 for aftershocks, 0 for mainshocks
- $Dip$  = Average dip of rupture plane (degrees)
- $W$  = Downdip rupture width (km)
- $V_{S30}$  = Average shear-wave velocity in top 30m of site profile (m/sec)
- $Z_{1.0}$  = Depth to 1.0 km/sec shear-wave velocity horizon (m)
- $Z_{2.5}$  = Basin (Sediment) depth; depth to 2.5 km/sec shear-wave velocity horizon (km)
- $Period$  = Spectral period for PSA (sec); 0 for PGA, -1 for PGV

Table 2 gives the predictor variables used by each developer team:

Table 2. Predictor variables in the GMPEs for each developer team.

Predictor variable	AS	BA	CB	CY
$M$	X	X	X	X
$R_{RUP}$	X		X	X
$R_{JB}$	X	X	X	X
$R_x$	X			X
$Z_{TOR}$	X		X	X
Fault type	X	X	X	X
$F_{AS}$	X			X
$Dip$	X		X	X
$W$	X			
$V_{S30}$	X	X	X	X
$Z_{1.0}$	X			X

$Z_{2.5}$			X	
Period	X	X	X	X

One thing to keep in mind is that the predictor variables can be correlated, and the effect of a variable not included in GMPEs can be captured by a variable in the equations with which it is correlated. A good example is  $V_{S30}$  and basin depth. Figure 4 shows that the two are correlated:

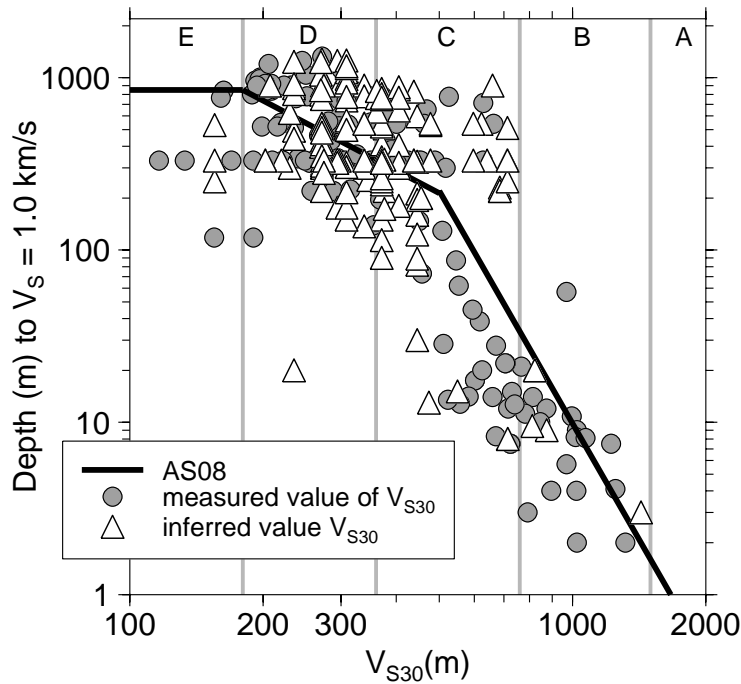


Figure 4. Correlation of depth of basin and  $V_{S30}$ .

Another example of correlations is given in Figure 5, which shows that fault type, magnitude, and depth-to-top of the rupture surface are correlated. In particular, note that few reverse-slip faults reach the surface, and that almost all earthquakes with magnitudes larger than 7.0 do reach the surface. Thus it might be difficult to unravel the physical effects associated with fault type, magnitude, or depth-to-top of rupture based on empirical analysis alone.

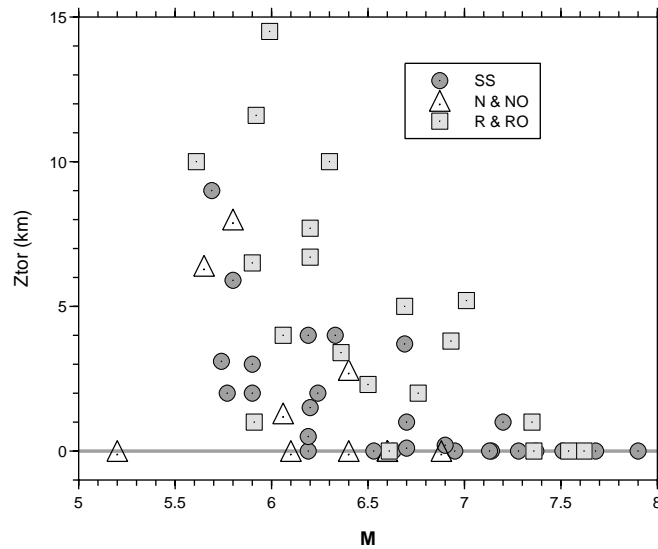


Figure 5. Correlation of fault type and magnitude with depth-to-top of rupture (SS: strike slip; N: normal; NO: normal oblique; R: reverse; RO: reverse oblique).

## Results

Figure 6 shows *PSA* at two periods from the BA GMPEs (the other GMPEs give similar results) as a function of distance for four magnitudes and a rock-like site. This figure shows the saturation with magnitude (which is larger for short periods than for long periods), as well as the stronger magnitude dependence at long periods than short periods.

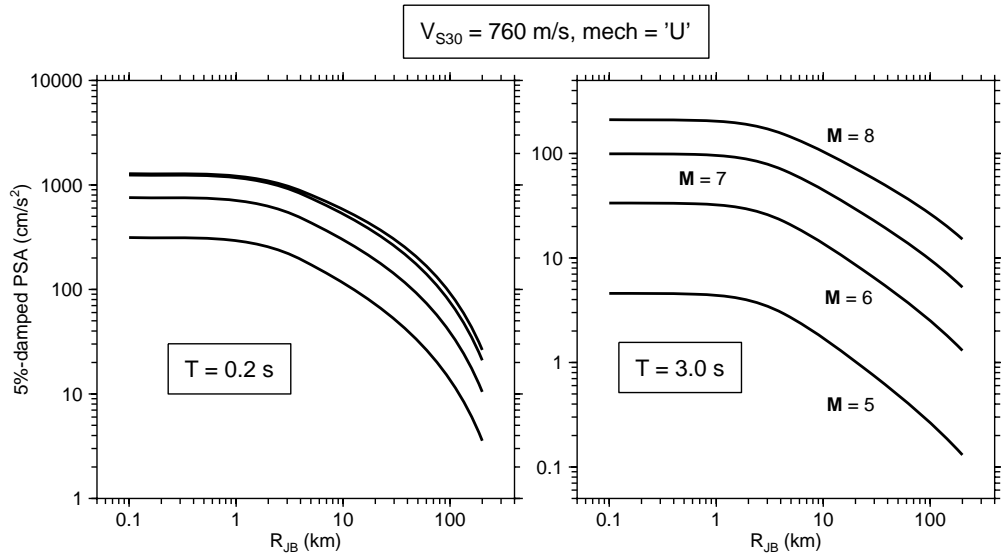


Figure 6. *PSA* vs. distance, from BA GMPEs.

The saturation with magnitude is also shown in Figure 7, which plots the average motions for each event, reduced to a common distance using the BA GMPEs, versus magnitude. This figure also shows the fault-type dependence of the motions.

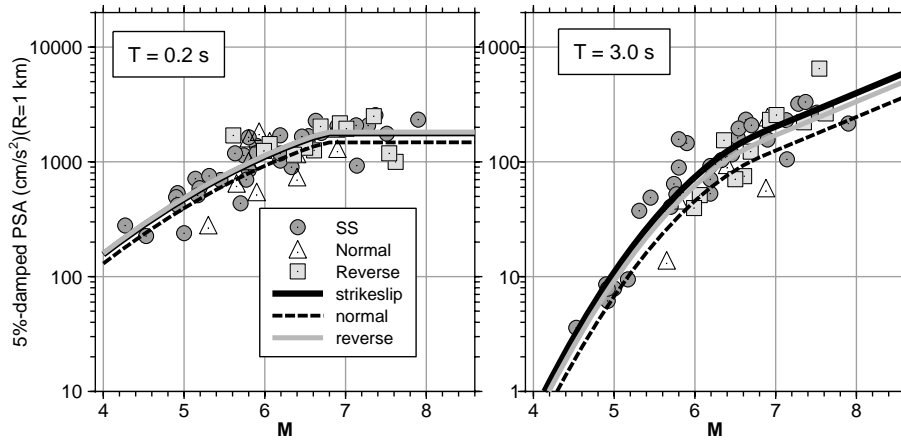


Figure 7. The symbols are average *PSA* for each event reduced to 1 km, using BA GMPEs, as a function of magnitude (one symbol per event). The curves show the magnitude dependence in the BA GMPEs.

The effect of site characterization is shown in Figure 8, again using the BA GMPEs. Note the effect of the nonlinear response, which results in a decrease in short-period motions on softer sites.

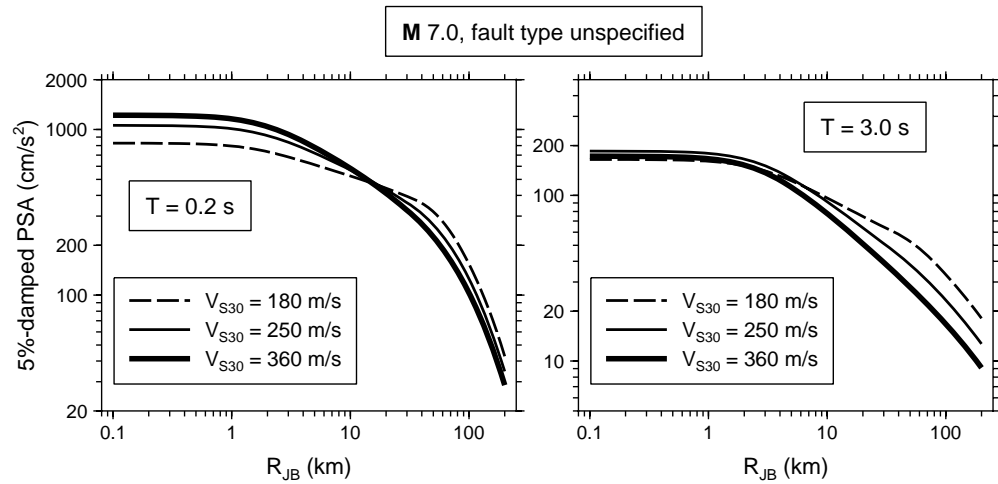


Figure 8. *PSA* vs. distance, from BA GMPEs.

A detailed comparison of the GMPEs for all NGA developer teams is given in Abrahamson et al. (2008). Here I show a few sample comparisons. Figure 9 compares the spectra as a function of period for strikeslip and reverse slip faults, for  $M 7$  and  $R_{JB} = 10$  km. In spite of the differences in datasets and functional forms, the different GMPEs give generally similar values of *PSA*, at least for the magnitude, distance, and site condition used for this figure (there can be larger differences for other distances, magnitudes, and site conditions).

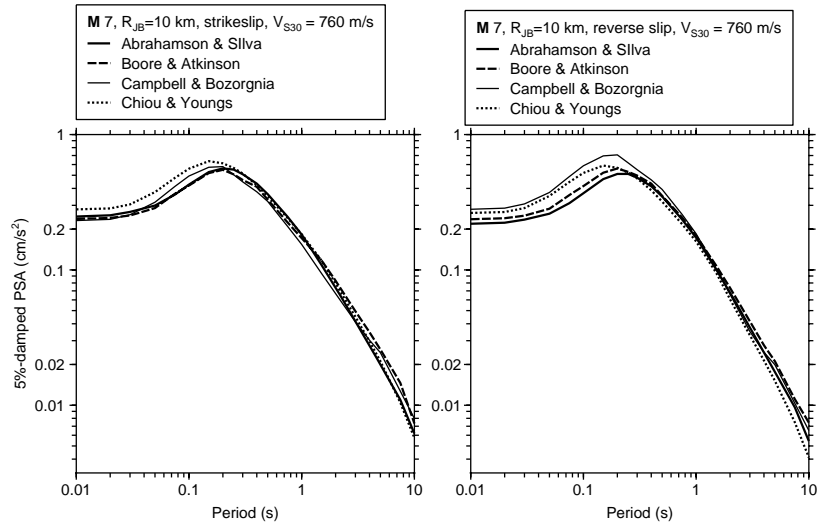


Figure 9. PSA vs. period.

One of the physical effects included in most of the GMPEs is the effect of being over the hanging wall of a fault (where observations and laboratory models suggest that the motions should be larger than for sites not over the hanging wall). Figure 10 shows the PSA for a 1 s oscillator for a scenario case, in which the fault extends at a 45 degree dip to the right, from the surface to a depth of 15 km (the fault crops out at 0 km distance).

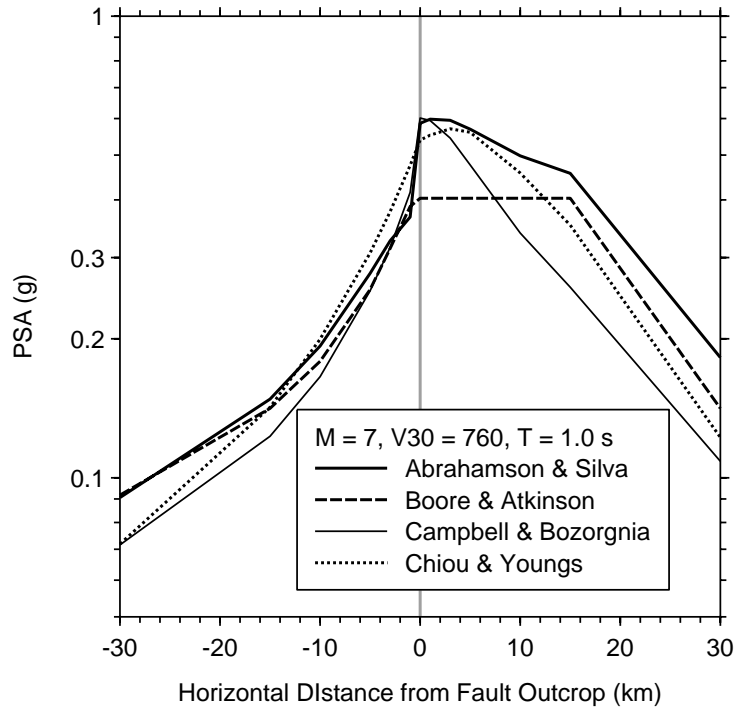


Figure 10. *PSA* vs. distance, for sites along a transect perpendicular to the fault strike, over the midpoint of a reverse-slip fault dipping at 45 degrees to the right, from 0 km depth to 15 km depth.

Another comparison of the NGA GMPEs is shown in Figure 11, which plots the event residuals as a function of magnitude (the residuals for the AS GMPEs were not available). Each symbol represents the average of the difference between observed and predicted motions for each event; the residuals for the 1999 Chi-Chi mainshock have been identified. These graphs show that the residuals have a similar scatter for the three GMPEs, but the values are not identical.

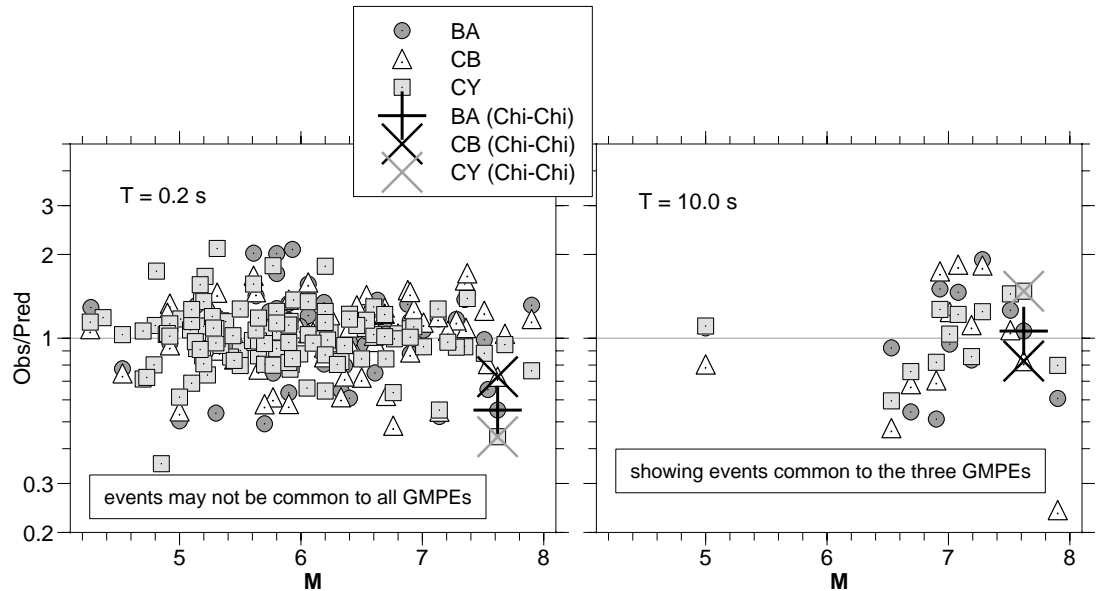


Figure 11. Event residuals (see text).

## Comparisons with Other Studies

A number of studies have compared motion from the NGA GMPEs with data generally different than used in the derivation of the NGA GMPEs. The first such comparison was by Stafford et al. (2008), who concluded “The analyses indicate that for most engineering applications, and particularly for displacement-based approaches to seismic design, the NGA models may confidently be applied within Europe.” Another study is that of Shoja-Taheri et al. (2010), who compare the ground motions from the NGA GMPEs with data from Iran; they find that the mean residuals (log observed – log predicted) are close to unity, indicating that the Iranian strong-motion data are consistent with the NGA GMPEs. In a third comparison, Bindi et al. (2010) showed that Italian strong-motion data are consistent with the NGA GMPEs. This is shown more quantitatively in Figure 12, which is redrafted from Scasserra et al. (2009). The bias for median ground motions (Fig. 12a) is generally close to zero for most of the NGA GMPEs.

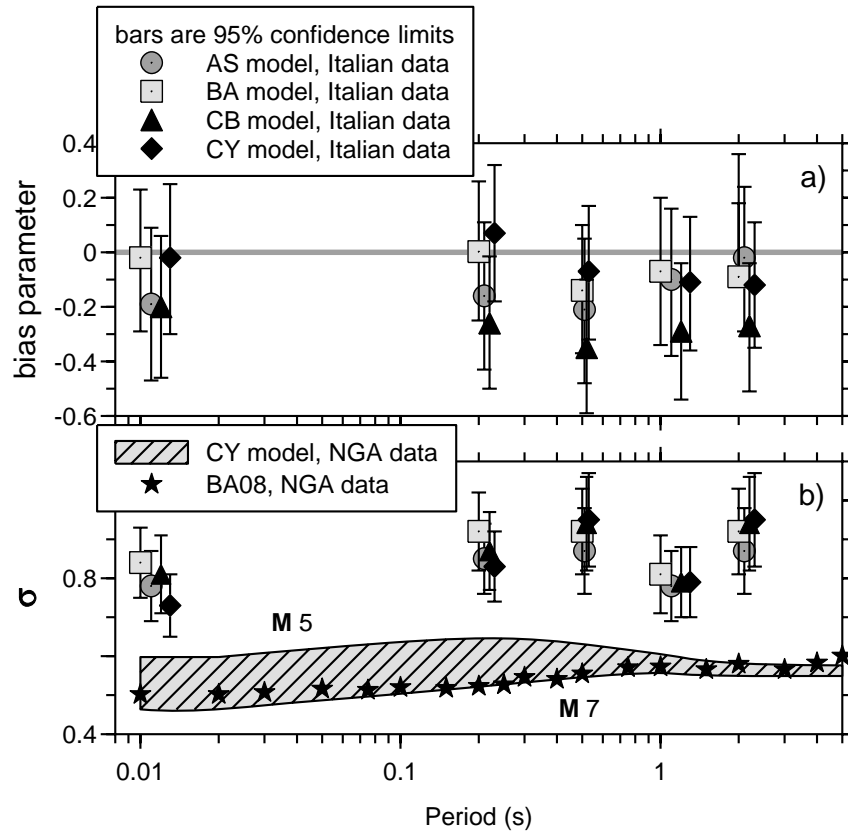


Figure 12. a) Bias in median ground motions between Italian strong-motion data and predictions from NGA GMPEs; b) Aleatory uncertainty for Italian data (relative to NGA GMPEs) and for the BA and CY GMPEs (the latter is magnitude dependent; shown are the values for magnitudes ranging from 5 to 7).

The standard deviation of Italian data is much higher than associated with the NGA GMPEs, as shown in Figure 12b (that figure also shows that the magnitude-independent aleatory uncertainty associated with the BA GMPEs is similar to the **M 7** aleatory uncertainty for the CY GMPEs). The uncertainties for the Italian data are relative to the NGA GMPEs because GMPEs for the Italian data were not available to the authors; the comparisons shown in Figure 12a suggest that similar results would have been obtained if GMPEs fit to the Italian data had been used.

## Conclusions

The NGA ground-motion prediction equations (GMPEs) are the result of an intensive multi-year project involving many participants. The equations were derived using a global dataset of ground motions from shallow crustal earthquakes in tectonically active regions. Comparisons with global data, most of which were not used in the development of the GMPEs, suggest that the equations are useful for predicting ground-motions for shallow crustal earthquakes in tectonically active regions worldwide.

## Acknowledgments

I thank Jon Stewart for providing the data used to construct Figures 12 and 13, and Sinan Akkar and Erol Kalkan for reviews of the paper.

## References

- Abrahamson, N., G. Atkinson, D. Boore, Y. Bozorgnia, K. Campbell, B. Chiou, I. M. Idriss, W. Silva, and R. Youngs (2008). Comparisons of the NGA ground-motion relations, *Earthquake Spectra* **24**, 45–66.
- Beyer, K. and J. J. Bommer (2006). Relationships between median values and between aleatory variabilities for different definitions of the horizontal component of motion, *Bull. Seismol. Soc. Am.* **96**, 1512–1522.
- Bindi, D., L. Luzi, M. Massa, and F. Pacor (2010). Horizontal and vertical ground motion prediction equations derived from the Italian Accelerometric Archive (ITACA), *Bull. Earthquake Eng.* **8**, (in press).
- Boore, D. M. and G. M. Atkinson (2007). Boore-Atkinson NGA Ground Motion Relations for the Geometric Mean Horizontal Component of Peak and Spectral Ground Motion Parameters, *PEER Report 2007/01*, Pacific Earthquake Engineering Research Center, University of California, Berkeley, 234 pp.
- Boore, D. M., J. Watson-Lamprey, and N. A. Abrahamson (2006). Orientation-independent measures of ground motion, *Bull. Seismol. Soc. Am.* **96**, 1502–1511.
- Campbell, K. W. and Y. Bozorgnia (2007). Campbell-Bozorgnia NGA Ground Motion Relations for the Geometric Mean Horizontal Component of Peak and Spectral Ground Motion Parameters, *PEER Report 2007/02*, Pacific Earthquake Engineering Research Center, University of California, Berkeley, 238 pp.
- Campbell, K., N. Abrahamson, M. Power, B. Chiou, Y. Bozorgnia, T. Shantz, and C. Roblee (2009). Next Generation Attenuation (NGA) project: empirical ground motion prediction equations for active tectonic regions, Sixth International Conference on Urban Earthquake Engineering, March 3-4, 2009, Tokyo Institute of Technology, Tokyo, Japan (available from [http://www.cuee.titech.ac.jp/Japanese/Publications/Doc/conference\\_6th.pdf](http://www.cuee.titech.ac.jp/Japanese/Publications/Doc/conference_6th.pdf)).
- Chiou, B., R. Darragh, N. Gregor, and W. Silva (2008). NGA project strong-motion database, *Earthquake Spectra* **24**, 23–44.

- Huang, Y.-N., A. S. Whittaker, and N. Luco (2008). Maximum spectral demands in the near-fault region, *Earthquake Spectra* **24**, 319—341.
- Lu, M., X. J. Li, J. X. Zhao (2010). A preliminary comparison of response spectra from the great 2008 Wenchuan earthquake in China with attenuation models developed for Japan and four NGA models, *Bull. Seismol. Soc. Am.* **100**, (submitted).
- Power, M., B. Chiou, N. Abrahamson, Y. Bozorgnia, T. Shantz, and C. Roblee (2008). An overview of the NGA Project, *Earthquake Spectra* **24**, 3--21.
- Scasserra, G., J. P. Stewart, P. Bazzurro, G. Lanzo, and F. Mollaioli (2009). A comparison of NGA ground-motion prediction equations to Italian data, *Bull. Seismol. Soc. Am.* **99**, 2961–2978.
- Shoja-Taheri, J., S. Naserieh, and H. Ghofrani (2010). A test of the applicability of NGA models to the strong ground-motion data in the Iranian Plateau, *J. Earthquake Engineering* **14**, 278--292.
- Stafford, P. J., F. O. Strasser, and J. J. Bommer (2008). An evaluation of the applicability of the NGA models to ground-motion prediction in the Euro-Mediterranean region, *Bull. Earthquake Eng.* **6**, 149–177.
- Watson-Lamprey, J. A. and D. M. Boore (2007). Beyond SaGMRotI: Conversion to  $Sa_{Arb}$ ,  $Sa_{SN}$ , and  $Sa_{MaxRot}$ , *Bull. Seismol. Soc. Am.* **97**, 1511—1524.